Biochimica et Biophysica Acta 1838 (2014) 438–444

Contents lists available at ScienceDirect

Biochimica et Biophysica Acta

journal homepage: www.elsevier.com/locate/bbamem

Reactive oxygen species at phospholipid bilayers: Distribution, mobility and permeation

Rodrigo M. Cordeiro *

Centro de Ciências Naturais e Humanas, Universidade Federal do ABC, Rua Santa Adélia 166, CEP 09210-170, Santo André (SP), Brazil

ARTICLE INFO

Article history:
Received 25 July 2013
Received in revised form 12 September 2013
Accepted 23 September 2013
Available online 1 October 2013

Keywords:
Antioxidant
Lipid peroxidation
Molecular dynamics simulation
Phospholipid bilayer
Free radical
Reactive oxygen species

ABSTRACT

Reactive oxygen species (ROS) are involved in biochemical processes such as redox signaling, aging, carcinogenesis and neurodegeneration. Although biomembranes are targets for reactive oxygen species attack, little is known about the role of their specific interactions. Here, molecular dynamics simulations were employed to determine the distribution, mobility and residence times of various reactive oxygen species at the membrane–water interface. Simulations showed that molecular oxygen (O_2) accumulated at the membrane interior. The applicability of this result to singlet oxygen ($^1O_2$) was discussed. Conversely, superoxide (O_2^-) radicals and hydrogen peroxide (H_2O_2) remained at the aqueous phase. Both hydroxyl (HO) and hydroperoxyl (HO_2) radicals were able to penetrate deep into the lipid headgroups region. Due to membrane fluidity and disorder, these radicals had access to potential peroxidation sites along the lipid hydrocarbon chains, without having to overcome the permeation free energy barrier. Strikingly, HO_2 radicals were an order of magnitude more concentrated in the headgroups region than in water, implying a large shift in the acid–base equilibrium between HO_2 and O_2^-. In comparison with O_2, both HO and HO_2 radicals had lower lateral mobility at the membrane. Simulations revealed that there were intermittent interruptions in the H-bond network around the HO radicals at the headgroups region. This effect is expected to be unfavorable for the H-transfer mechanism involved in HO diffusion. The implications for lipid peroxidation and for the effectiveness of membrane antioxidants were evaluated.

1. Introduction

Reactive oxygen species (ROS) are of primary importance in a large number of contemporary research topics in Chemistry and Biology, as for instance photocatalysis [1], environmental Chemistry [2] and nanotoxicity [3]. In the organism, ROS are naturally present and participate in redox signaling pathways that are essential for the physiological control of cell function [4]. However, they are also involved in deleterious processes such as aging, carcinogenesis and neurodegenerative diseases [4–6].

Highly reactive superoxide (O_2^-) and hydroperoxyl (HO_2) radicals are generated by the mitochondrial electron transport chain. To cope with their toxicity, the organism produces superoxide dismutases that convert O_2^- into the less reactive hydrogen peroxide (H_2O_2). However, in the presence of trace metals, H_2O_2 may generate highly toxic hydroxyl radicals (HO) via Fenton-type reactions [7,8]. In addition, artificially generated singlet oxygen ($^1O_2$) plays a central role in the anti-cancer treatment known as photodynamic therapy [9].

Biomembranes are very susceptible to the attack by biologically or photodynamically generated ROS [10–12]. The presence of oxidized lipids is able to change membrane properties, especially with regards to permeability [13–16]. From a mechanistic point of view, the distribution of different ROS at the biomembrane–water interface is crucial for the understanding of their reactions in the organism, including lipid peroxidation and radical scavenging by membrane antioxidants. Up to now, experiments have been able to provide a qualitative panorama of these issues using spin traps and fluorescent probes as reporters for ROS penetration into lipid bilayers [17–19]. Results are usually associated with large uncertainties because molecular probes are mobile and cannot be precisely located in the membrane, as recently demonstrated by computer simulations [20].

Molecular modeling studies have offered the first insights about the behavior of ROS close to interfaces. They have shown that certain water-soluble oxy-radicals accumulate at the air–water interface of droplets [21–24]. In addition, H_2O_2 was found to accumulate at the surface of proteins [25,26]. Recently, the reactions between ROS and bacterial cell walls have been considered theoretically [27]. Little is still known, however, about the interactions between ROS and phospholipid membranes [28]. Experiments show that the accumulation of molecular oxygen (O_2) and nitric oxide (NO) inside a phospholipid bilayer leads to the magnification of their reaction rates, the so-called "membrane lens effect" [29]. Analogously, both experiments [30] and simulations [31] indicate that the $^1O_2$ generation efficiency of photosensitizers increases proportionally to their degree of accessibility to the oxygen-rich membrane interior. There are several studies about the partitioning

* Tel.: +55 11 49960173.
E-mail address: rodrigo.cordeiro@ufabc.edu.br.

0005-2736/$ – see front matter © 2013 Elsevier B.V. All rights reserved.
http://dx.doi.org/10.1016/j.bbamem.2013.09.016

behavior of simple molecules at phospholipid bilayers [32–36]. However, no systematic study is available for a wider variety of biologically and therapeutically relevant ROS.

In the work presented here, molecular dynamics simulations were employed to calculate the distribution, mobility and residence times of various ROS at the phospholipid–water interface. Purely classical models allow for the study of the partition behavior alone, without chemical reactions. The following species were investigated: O_2^-, HO_2, H_2O_2, HO and O_2 (with results extended to $^1O_2$). Results showed that these ROS had significantly different tendencies for penetration and accumulation at the surface of phospholipid membranes. The implications for lipid peroxidation and for the effectiveness of membrane antioxidants were evaluated based on a molecular view of the interactions between ROS and phospholipids.

2. Simulation methods

2.1. Simulation setup

Molecular dynamics (MD) simulations [37,38] were performed using a single precision version of the GROMACS 4.5.1 package [39,40]. To integrate Newton's equations of motion, a leapfrog Verlet scheme [37,38] was used with a time step of 2 fs. Periodic boundary conditions were considered in all Cartesian directions. In the following, a summarized description of the simulation protocols is provided. Further technical details can be found as supplementary data.

2.2. Derivation of interaction parameters

Fully hydrated lipid bilayers of 2-oleoyl-1-palmitoyl-*sn*-glycero-3-phosphocholine (POPC) were represented using the parameters of Poger and Mark [41] and the SPC water model [42]. These parameters were demonstrated to lead to membrane structural properties that are consistent with experiments. Accordingly, molecular interactions were described in the framework of the GROMOS 53A6 force field [43]. This force field is suitable for describing partitioning phenomena because molecular interactions are empirically adjusted to reproduce solvation free energy data. Parameters for bonds, angles and torsions were adapted from the literature for O_2^-, HO_2, H_2O_2, HO and O_2 [44–47]. van der Waals interactions and partial charges were adjusted to simultaneously reproduce pure liquid properties of H_2O_2 [48] and the experimental hydration free energies of various ROS [49]. The van der Waals interactions of O_2 were adjusted to simultaneously reproduce its solvation free energy in water and cyclohexane [50,51]. As noted in a previous work [52], the inversion of one electronic spin in the transition from ground-state O_2 to its singlet-type excited state is not explicitly considered in purely classical molecular mechanical models. For this reason, both species were here described with the same set of parameters and were not distinguished from each other. This assumption is motivated by experimental evidence that indicates that these species have similar partition coefficients between water and hydrophobic media [53–56].

The thermodynamic integration (TI) method [37,38,57] was employed for the calculation of solvation free energies. In this method, the solute is removed from the system by scaling down to zero all solute–solvent interactions in a stepwise manner as function of a coupling parameter λ. The free energy variation is obtained by integration of the average value of the derivative of the total Hamiltonian with respect to λ. Single ROS molecules were solvated in cubic water boxes with ca. 3 nm length. Coulomb and Lennard-Jones interactions were decoupled sequentially using 21 and 51 evenly spaced steps, respectively. Each step involved a 600 ps pre-equilibration phase, followed by 5 ns of data acquisition in the isothermal-isobaric (NPT) ensemble at 298 K and 1 bar. The interaction parameters obtained are listed in Table S1 and their derivation is fully documented in Figs. S1, S2 and S3.

2.3. Permeation free energy profiles

With the partial charges derived from TI, the free energy profiles for ROS translocation across POPC bilayers were calculated using the umbrella sampling (US) method [58]. Starting structures for US were picked randomly from the last 50 ns of a 100 ns simulation of a hydrated bilayer containing 128 lipid molecules. The simulated systems had lateral dimensions of ca. 6.2 nm parallel to the membrane surface (*xy*-plane) and ca. 8.5 nm along the bilayer normal (*z*-axis). A total of 144 umbrella windows separated by 0.5 Å were defined along the *z*-axis, so as to span the whole bilayer thickness region up to bulk water. ROS were inserted at the centers of umbrella windows by gradually switching on their interactions with the rest of the system during 100 ps. Although ROS were free to move in the *xy*-plane, motion was restricted along the *z*-axis by a harmonic bias with a force constant of 1000 $kJ \cdot mol^{-1} \cdot nm^{-2}$. After a pre-equilibration period of 500 ps, the collection of umbrella histograms took place for 2 ns in the NPT ensemble at 310 K and 1 bar. Under these conditions, the POPC bilayer was in its fluid liquid-crystalline state. Free energy profiles were built by the weighted histogram analysis method (WHAM) [58] using the g_wham tool [59]. Final results for each ROS were obtained by the average of four independent US simulations.

2.4. Simulations of ROS distribution and dynamics

To study the behavior of ROS at the membrane–water interface, 30 molecules of each of the non-ionic ROS were initially placed together at the aqueous phase surrounding a pre-equilibrated bilayer. This corresponded to an initial molar fraction of ca. 0.5% for each ROS at the aqueous phase. This value is still orders of magnitude higher than experimentally measured ROS concentrations in mitochondria [60]. However, it provides reasonable statistics [61]. After 20 ns of equilibration, data acquisition followed for 30 ns in the NPT ensemble at 310 K and 1 bar. Since ions are known to affect the membrane lateral packing [62], a separate simulation was performed for 30 O_2^- ions in the presence of Na^+ counterions. Density profiles were built along the *z*-direction to determine the ROS distribution at the membrane–water interface. The residence times of ROS at the lipid headgroups region were determined in terms of survival time correlation functions, as introduced by Impey et al. [25,63]. In addition, a POPC bilayer was simulated in the presence of the antioxidants β-carotene, α-tocopherol and Trolox® (chemical structures in Fig. S4). The interaction parameters of membrane additives were pieced together from the GROMOS 53A6 library by analogy with existing structures and functional groups. Longer simulations (150 ns) were performed to equilibrate these systems. Molecular topology files describing the structure and interactions of ROS and antioxidants are available as supplementary data.

3. Results and discussion

3.1. Distribution of ROS at the membrane–water interface

Fig. 1 shows the partitioning behavior of ROS between the aqueous phase and a POPC bilayer, as obtained from MD simulations. The free energy profiles for ROS translocation across the membrane (Fig. 1A) were consistent with independent simulations of the equilibrium ROS distributions in the system (Fig. 1B). In the case of hydrophobic O_2 molecules, the free energy had a minimum at the bilayer center and there was no significant energy barrier for permeation. On average, O_2 was ca. 3.5 times more concentrated in the membrane interior than in bulk water, in line with experimental measurements [64]. Following the assumptions discussed in Section 2.2, $^1O_2$ is expected to behave in a similar fashion. For all hydrophilic ROS, the membrane acted as a permeation barrier. These results are supported by experimental evidence that species such as HO_2 and H_2O_2 are much less permeant than O_2 [28]. In the case of H_2O_2, a shallow free energy minimum appeared at the headgroups region due to favorable H-bond interactions with

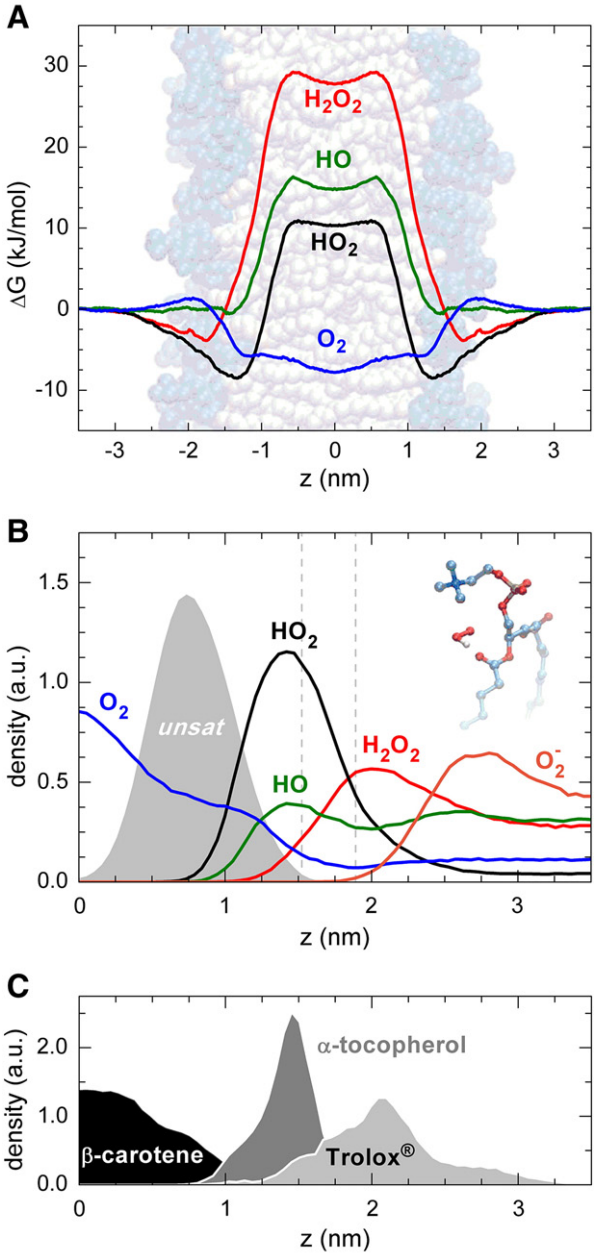

Fig. 1. (A) Symmetrized free energy profiles for the translocation of various ROS across a POPC bilayer (background image). (B) Distribution of different ROS (full lines) and lipid unsaturations (*unsat*, shaded) along the bilayer normal. Distances are expressed in relation to the bilayer center ($z = 0$). Vertical dashed lines indicate the average positions of carbonylester ($z = 1.52$ nm) and the phosphate ($z = 1.89$ nm) groups. The inset shows the H-bond formed between a HO_2 radical and a carbonylester group. (C) Distributions of the conjugated chains of β-carotene (black) and the hydroxyl groups of α-tocopherol (dark gray) and Trolox® (light gray).

phosphate groups. The activation free energy for H_2O_2 permeation was estimated in 33 ± 4 kJ/mol (see Fig. S5 for an uncertainty analysis), in agreement with the value of 36.8 kJ/mol found experimentally [65].

Significantly lower barriers were found for HO and HO_2 radicals. As shown in Table 1, hydrophilic ROS may act as both H-bond donors and acceptors in water. However, H_2O_2 establishes about twice as many H-bonds in water as HO or HO_2. In comparison to H_2O_2, these radicals were more prone to lose their hydration waters and penetrate into the headgroups region. The loss of two H-bonds per radical in water was partly compensated by the formation of an H-bond with a lipid carbonylester group, with the radical acting as an H-bond donor.

Table 1
H-bonds between ROS and water.

Species	Number of H-bonds[a]	
	(As donor)	(As acceptor)
H_2O_2	1.9	2.6
HO_2	1.0	0.8 (central O) 0.5 (lateral O)
HO	1.0	1.0

[a] H-bonds were defined based on a maximum H-acceptor distance of 2.5 Å and a maximum H-donor–acceptor angle of 30°.

The HO_2 radical was found to accumulate at the interface. The free energy profile of HO_2 exhibited a deep free energy minimum at the headgroups region, with a value of −8.5 kJ/mol relative to the aqueous phase. In the HO_2 distribution, a concentration enhancement of more than one order of magnitude was observed at the headgroups region. The ratio between the surface and bulk concentrations in this region is consistent with the concentration enhancement expected from the free energy minimum, as obtained at infinite dilution. As demonstrated in Fig. S6, the difference in the behavior of HO and HO_2 radicals can be explained by the presence of one additional oxygen atom in HO_2, which led to stronger van der Waals interactions with the lipid headgroups. To rule out the presence of force field artifacts, simulations were repeated using different parameters for the headgroups and qualitatively similar results were obtained (see Fig. S7).

The peculiar behavior of each ROS will probably have implications for the efficiency of radical scavengers. To illustrate this point, Fig. 1C shows how commonly used antioxidants were distributed in a hydrated POPC bilayer (chemical structures are displayed in Fig. S4). Molecules of β-carotene, a hydrophobic antioxidant, had easier access to species that also accumulated in the membrane interior, as was the case of O_2. Conversely, hydrophilic molecules of Trolox® had easier access to water-soluble species. Molecules of α-tocopherol, with their amphiphilic structure, accumulated at the membrane–water interface, where they had greater accessibility to non-ionic hydrophilic ROS, especially HO_2. In fact, carotenoids are known for their efficiency as $^1O_2$ quenchers in biological systems, an effect that can be partly attributed to the tendency of these molecules to accumulate in the membrane interior. A relationship between the partition constant of several antioxidants and the $^1O_2$ quenching rates has been experimentally demonstrated [66].

Another implication of the partitioning behavior of the various ROS relates to chemical reactions with the phospholipids themselves. Fig. 1 suggests that certain hydrophilic ROS do not need to overcome their permeation free energy barrier in order to have access to the lipid hydrocarbon chains, where lipid peroxidation takes place. Due to membrane fluidity and disorder, there was a significant overlap between the distributions of HO and HO_2 radicals and the distribution of the unsaturations at lipid oleoyl chains. The same effect is expected to be relevant in experiments that rely on molecular probes to detect ROS at different immersion depths within the membrane [17–19]. Even when these probes are covalently attached to the lipid hydrocarbon chains, their reactions with ROS will depend not only on their average position along the membrane normal, but also on the width of their distribution. Therefore, it is convenient to calculate the probability of molecular encounters between ROS and lipid segments by means of the integral overlap of the distributions of the species involved. This probability (P) is given by:

$$P_i \propto \frac{1}{\rho_{ROS}^{\infty}} \int dz \rho_i(z) \cdot \rho_{ROS}(z), \quad (1)$$

where $\rho_i(z)$ is the distribution of the ith carbon atom of the lipid acyl chains and $\rho_{ROS}(z)$ is the distribution of a specific ROS. The integral runs over the whole system length along the membrane normal. In

order to compare different species, the probability needs to be normalized by the ROS concentration in bulk water, here represented as ρ^{∞}_{ROS}.

The relative probabilities of contacts between ROS and different sections of the lipid acyl chains are depicted in Fig. 2A and B. For the hydrophobic O_2, the probability increased from the headgroups to the tail region. Almost the opposite happened to hydrophilic ROS, with the exception that the probability minimum was not at the tail end. Both O_2 and HO_2 had the largest degree of accessibility to the double bond region. In the context of lipid peroxidation, double bonds are very susceptible to the attack by $^1O_2$ [11]. In turn, HO_2 radicals are able to generate lipid radicals by abstracting bisallylic hydrogen atoms from polyunsaturated non-conjugated lipids [67]. The accessibility of the HO radical to the double bond region was found to be more than one order of magnitude lower in comparison with O_2. Still, the importance of HO to lipid peroxidation should not be undermined because this radical is 5 orders of magnitude more reactive toward lipids than $^1O_2$ [11].

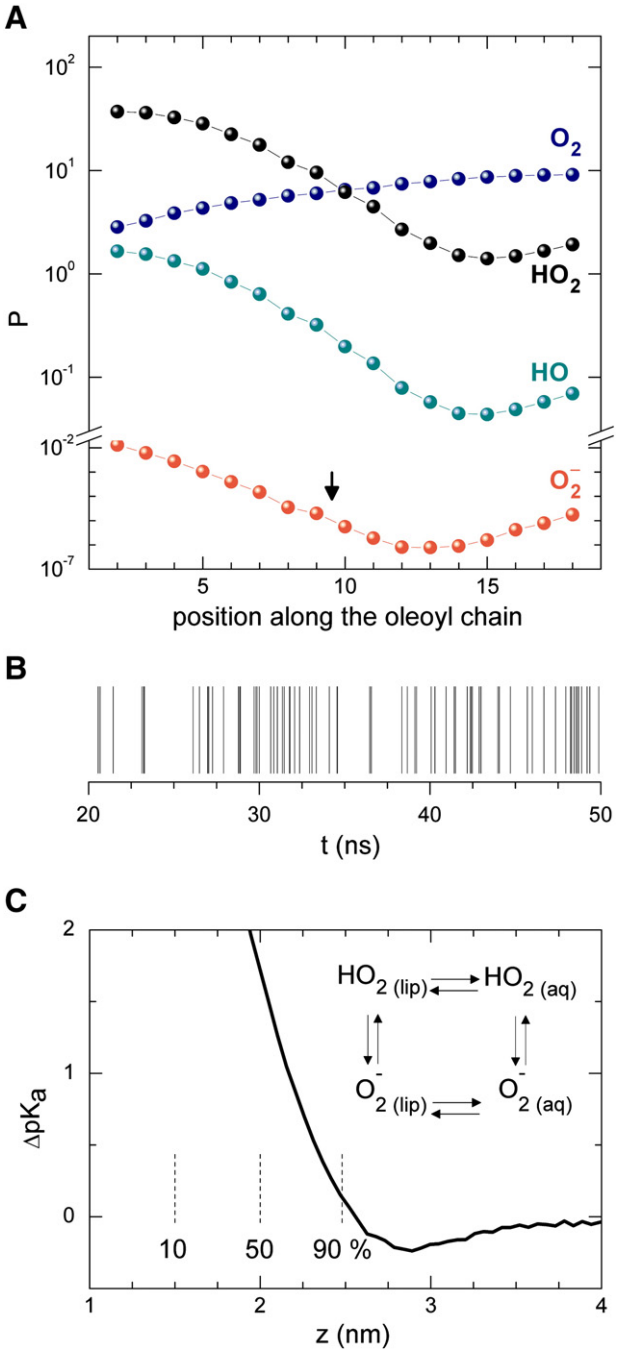

Fig. 2. (A) Relative probabilities of contacts between ROS and carbon atoms along the phospholipid oleoyl chains. Carbon atoms are numbered from 1 (carbonyl) to 18 (last tail atom). The arrow indicates the position of the unsaturation. (B) Contacts between HO_2 radicals and the allylic carbons of the lipid oleoyl chains. Vertical black lines indicate instants in which contacts were established with appropriate geometries for H-abstraction reactions. (C) Change in the pKa value of HO_2 as function of the distance to the bilayer center. The assumptions needed for the calculation are explained in the text. Vertical dashed lines indicate the relative decrease in the density of water at the interface with respect to the bulk value. The inset shows the thermodynamic cycle used for the calculation of the pKa shift in the lipid (lip) phase.

Among all the ROS investigated, O_2^- radicals had the lowest probability to establish molecular contacts with hydrocarbon chains. However, due to membrane fluidity and disorder, there was a nonzero overlap even between the distributions of the last atoms of the lipid tails and the O_2^- radicals (see Fig. S8). Clearly, these values should be considered as qualitative due to limited sampling of O_2^- configurations at the headgroups region and to membrane undulations. According to experimental evidence, the importance of O_2^- for lipid peroxidation is fundamented rather on its ability to form HO_2 in aqueous solution [68–70]. In fact, the HO_2 radical is the conjugated acid of O_2^-, with a pKa of 4.7 [71]. At physiological pH, however, only ca. 0.2% of all O_2^- is in the protonated form. Nevertheless, simulation results indicate that the degree of accessibility of HO_2 to the double bond region is about 5 orders of magnitude higher in comparison with O_2^-. It implies that the protonated acid, although far from being the predominant species, is still able to reach the peroxidation site with higher probability than O_2^- itself. In this context, the possible role of HO_2 in lipid peroxidation naturally emerges as a consequence of its pronounced accumulation in the lipid headgroups region.

Using the thermodynamic cycle in Fig. 2C, this effect was expressed in terms of a position dependent pKa shift. First, the HO_2 distribution was scaled down so as to reproduce the correct acid/base ratio in bulk water at physiological pH. Then, the change in the acid–base equilibrium constant was estimated based on the ratio between the concentrations of HO_2 and O_2^-. It was assumed that the pH did not vary with distance and that the lipid headgroups region remained sufficiently hydrated so that solvent effects could be neglected in the pH definition. According to Fig. 2C, under these assumptions, a pKa increase of more than one unit was obtained at the headgroups region. It should be emphasized, however, that the sampling of O_2^- configurations at the headgroups region was itself insufficient for an accurate prediction of the pKa shift. Therefore, the results in Fig. 2C must be considered qualitatively.

3.2. Dynamics of ROS at the membrane–water interface

Fig. 3 shows the dynamics of various ROS at the membrane–water interface. As depicted in Fig. 3A, O_2 remained most of the time within the hydrophobic membrane interior, with only sporadic and short excursions to the aqueous phase. All hydrophilic ROS were able to visit the headgroups region and to return to the aqueous phase. Due to specific interactions with the carbonylester groups, HO_2 radicals stayed adsorbed for the longest time.

Statistically, the dynamics of adsorption/desorption was evaluated by means of a survival time correlation function $f(t)$ (see Eq. S5) [25,63]. Given a certain number of molecules initially adsorbed at the membrane surface, the function $f(t)$ quantifies which fraction of these molecules remains adsorbed without ever leaving after an interval of time t. In all cases, a distance of 2.5 nm was chosen as the boundary between the bilayer and the aqueous phase. As displayed in Fig. 3B, the function $f(t)$ exhibited a short timescale decay associated with fast boundary recrossing processes. At longer timescales, a slower exponential decay associated with desorption was observed. The residence time was considered as the decay constant of the longer timescale process. In the specific case of O_2, the residence time did not refer to adsorption/desorption but to partitioning between the aqueous phase and the membrane.

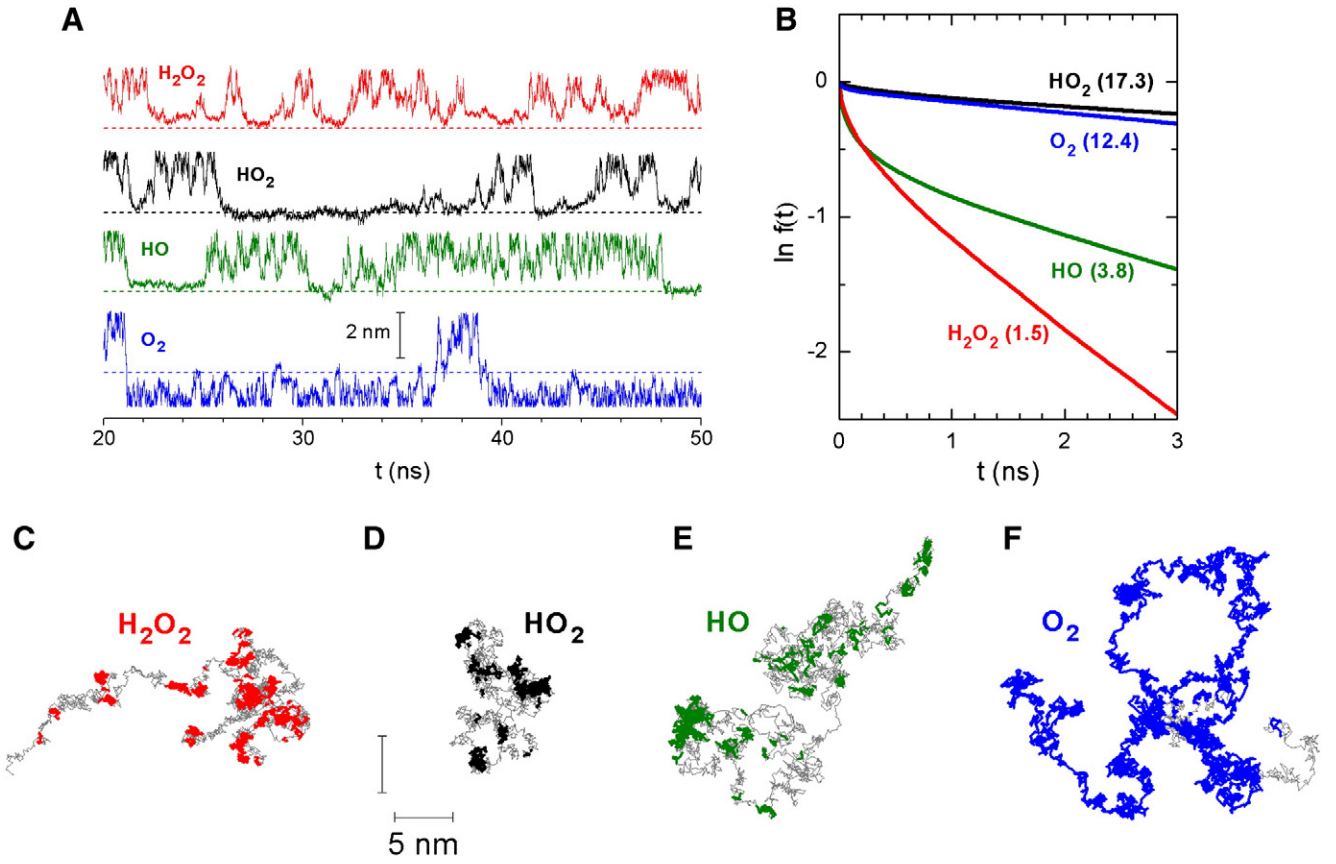

Fig. 3. (A) Distances between selected individual molecules and the bilayer center as function of time. Horizontal dashed lines indicate the average position of the carbonylester groups at $z = 1.52$ nm. (B) Survival correlation functions related to ROS adsorption/desorption. The values in parenthesis are the residence times at the phospholipid headgroups region, reported in units of ns. (C–F) Trajectories of different ROS, showing their lateral mobility parallel to the membrane surface. Thin gray lines refer to motion in the aqueous phase, while colored bold lines refer to motion at the headgroups region or in the membrane interior.

Both O_2 (and probably $^1O_2$ by analogy) and HO_2 were associated with the longest residence times, which were 12.4 and 17.3 ns, respectively. However, the half-life of these species is typically orders of magnitude larger [11]. It means that, if they are locally generated at the membrane, they have a considerable chance to escape to the aqueous phase without reacting with the phospholipids. In contrast to that, HO radicals were associated with a residence time of ca. 3.8 ns, while their typical lifetime is of the order of 1 ns. To cause membrane damage, these radicals need to be generated very close to the membrane surface. However, once generated there, they will almost certainly react with the lipids. Both HO_2 and HO radicals were able to establish long-lived H-bonds with the membrane carbonylester groups. As demonstrated in Fig. 3C–F, this led to a severe impairment of their lateral mobility in comparison with O_2.

Although simulations provided important clues about the partition and dynamics of ROS at the membrane–water interface, attention must be called to a few limitations. Especially in the case of short-lived radicals such as HO, the competing processes of radical generation and scavenging are likely to give rise to a steady-state rather than an equilibrium distribution over larger distances. Besides that, reactivity is influenced not only by ROS accumulation, but also by the activity within the lipidic environment, which may differ from that in the aqueous bulk. The reactivity of antioxidants toward ROS is supposed to depend also on the local dielectric constant, which varies as function of the immersion depth in the membrane [72]. Furthermore, details of electronic structure, such as for instance the difference between singlet and triplet oxygen, are not explicitly considered in classical models. By the other side, electronic structure calculations are limited with regards to the time and length scales accessible. It is not possible to neglect the importance of quantum effects that lead to chemical reaction and influence radical mobility. As demonstrated by hybrid quantum mechanical/molecular mechanical methods, the diffusion of HO radicals in aqueous solution occurs via H-transfer reactions with solvent molecules [73].

Even in this respect, however, purely classical simulations are able to make qualitative predictions. The images in Fig. 4 are simulation snapshots showing a HO radical bound as an H-bond donor to one of the carbonylester groups of a phospholipid. They reveal the existence of an H-bond network that links the HO radical to the bulk aqueous solution. The maintenance of this network is a pre-requisite for the occurrence of an H-transfer mechanism. It was found, however, that this H-bond network disappeared intermittently. It was completely absent during most of the time during which the radical remained attached to the carbonylester group. The loss of hydration suffered by HO upon penetration into the headgroups region is expected to hamper the H-transfer mechanism, contributing to the decrease of the lateral mobility of this radical along the membrane surface.

4. Conclusions

The results obtained from molecular dynamics simulations offer a basis for the interpretation of experiments of membrane peroxidation induced by ROS. It was demonstrated, for instance, that even hydrophilic species such as HO and HO_2 radicals were able to penetrate deep into the lipid headgroups region. Due to membrane fluidity and disorder, these radicals had access to potential peroxidation sites along the lipid hydrocarbon chains, without having to overcome the permeation free energy barrier. In a similar fashion, hydrophilic ROS had easier access to amphiphilic and hydrophilic antioxidants, here represented by α-tocopherol and Trolox®, respectively. In turn, hydrophobic β-carotene molecules had more access to hydrophobic species that also accumulated in the

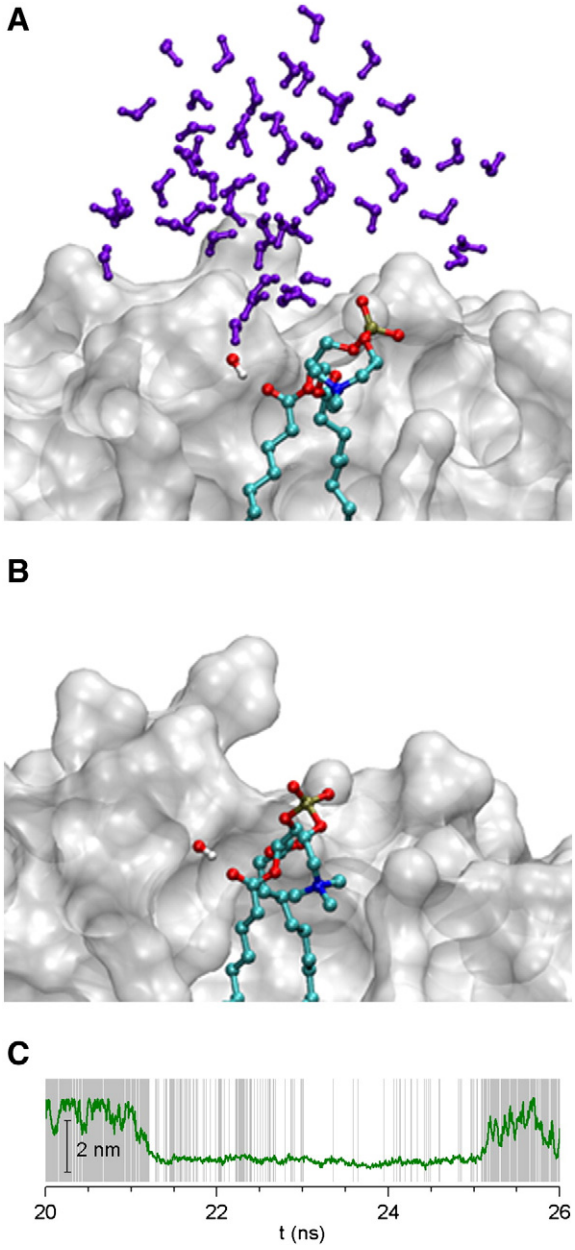

Fig. 4. Simulation snapshots showing a HO radical at the phospholipid headgroups region at (A) 21.535 and (B) 23.235 ns. The HO radical and the nearest phospholipid are represented according to the following color coding: C (cyan), H (white), N (blue), O (red), P (brown). The rest of the bilayer is represented in gray. The water molecules involved in an H-bond network with the HO radical are represented in purple up to the 10th generation. (C) Penetration depth of the HO radical as function of time. Shaded regions indicate instants in which an H-bond existed between HO and water.

membrane interior, such as O_2 and presumably $^1O_2$ as well. All results were obtained for phosphatidylcholine, which is a major component of biological membranes. Further investigations will be performed about different lipid types and the influence of cholesterol.

Up to now, the role of HO_2 in lipid peroxidation has received minor attention because, at physiological pH, this species exists almost exclusively in the form of its conjugated base O_2^-. However, different from all other ROS, HO_2 radicals were found to be one order of magnitude more concentrated in the headgroups region than in bulk water. It represents an increase of more than one order of magnitude in the acid/base equilibrium constant involving HO_2 and O_2^-. Simulations indicated that, even at physiological pH, HO_2 may have an important role in the context of both lipid peroxidation and radical scavenging by membrane antioxidants.

The residence times of HO_2 and HO radicals at the membrane–water interface were 17.3 and 3.8 ns, respectively, in comparison with a residence time of 12.4 ns found for O_2 in the membrane interior. Both oxy-radicals were involved in long-lived H-bonds with the membrane carbonylester groups, which led to a severe impairment of their lateral mobility along the membrane surface in comparison with O_2. Simulations revealed that, due to limited hydration at the headgroups region, there were intermittent interruptions in the H-bond network connecting HO radicals to bulk water. These interruptions are expected to decrease HO mobility by hampering the H-transfer mechanism. Even then, the mobility predicted by purely classical methods is expected to be underestimated because it does not account for the H-transfer process, which is expected to take place at least intermittently at the membrane surface. Taken together, the insights obtained from simulations may ultimately contribute to a better understanding of oxidative stress mechanisms at the molecular level.

Acknowledgements

This work was made possible thanks to fruitful discussions with Luis G. Dias, Mauricio D. C. Neto, Maurício S. Baptista and Ronei Miotto. The scientific computing section of Universidade Federal do ABC is acknowledged for the computational resources and technical support. The São Paulo Research Foundation (FAPESP) is acknowledged for the financial support (grant no. 2012/50680-5).

Appendix A. Supplementary material

Further details about simulation methods. Derivation of partial charges (Fig. S1). Comparison between calculated and experimental solvation free energies of ROS (Fig. S2). Force field parameters for ROS (Table S1). Radial distribution functions showing ROS hydration (Fig. S3). Chemical structures of POPC and antioxidants (Fig. S4). Non-symmetrized free energy profiles and the associated uncertainties (Fig. S5). Interactions between ROS and phospholipids at the headgroups region (Fig. S6). Force field sensitivity test (Fig. S7). Distributions of lipid tail atoms (Fig. S8). Molecular topologies of ROS and antioxidants (separate files). Supplementary data to this article can be found online at doi: http://dx.doi.org/10.1016/j.bbamem.2013.09.016.

References

[1] W. Macyk, A. Franke, G. Stochel, Metal compounds and small molecules activation — case studies, Coord. Chem. Rev. 249 (2005) 2437–2457.
[2] M.O. Andreae, P.J. Crutzen, Atmospheric aerosols: biogeochemical sources and role in atmospheric chemistry, Science 276 (1997) 1052–1058.
[3] D. Napierska, L.C.J. Thomassen, D. Lison, J.A. Martens, P.H. Hoet, The nanosilica hazard: another variable entity, Part. Fibre Toxicol. 7 (2010) 39.
[4] W. Dröge, Free radicals in the physiological control of cell function, Physiol. Rev. 82 (2002) 47–95.
[5] B. Halliwell, J.M.C. Gutteridge, Oxygen toxicity, oxygen radicals, transition metals and disease, Biochem. J. 219 (1984) 1–14.
[6] A. Sanz, R. Pamplona, G. Barja, Is the mitochondrial free radical theory of aging intact? Antioxid. Redox Signal. 8 (2006) 582–599.
[7] J. Prousek, Fenton chemistry in biology and medicine, Pure Appl. Chem. 79 (2007) 2325–2338.
[8] Z. Cheng, Y. Li, What is responsible for the initiating chemistry of iron-mediated lipid peroxidation: an update, Chem. Rev. 107 (2007) 748–766.
[9] S.B. Brown, E.A. Brown, I. Walker, The present and future role of photodynamic therapy in cancer treatment, Lancet Oncol. 5 (2004) 497–508.
[10] A.W. Girotti, Photosensitized oxidation of membrane lipids: reaction pathways, cytotoxic effects, and cytoprotective mechanisms, J. Photochem. Photobiol. B Biol. 63 (2001) 103–113.
[11] K.M. Schaich, Lipid oxidation: theoretical aspects, in: F. Shahidi (Ed.), Bailey's Industrial Oil and Fat Products, Wiley, 2005, pp. 269–355.
[12] E. Schnitzer, I. Pinchuk, D. Lichtenberg, Peroxidation of liposomal lipids, Eur. Biophys. J. 36 (2007) 499–515.
[13] J. Wong-Ekkabut, Z. Xu, W. Triampo, I.-M. Tang, D.P. Tieleman, L. Monticelli, Effect of lipid peroxidation on the properties of lipid bilayers: a molecular dynamics study, Biophys. J. 93 (2007) 4225–4236.
[14] P.T. Vernier, Z.A. Levine, Y.-H. Wu, V. Joubert, M.J. Ziegler, L.M. Mir, D.P. Tieleman, Electroporating fields target oxidatively damaged areas in the cell membrane, PLoS ONE 4 (2009) e7966.

[15] L. Beranova, L. Cwiklik, P. Jurkiewicz, M. Hof, P. Jungwirth, Oxidation changes physical properties of phospholipid bilayers: fluorescence spectroscopy and molecular simulations, Langmuir 26 (2010) 6140–6144.
[16] V. Jarerattanachat, M. Karttunen, J. Wong-ekkabut, Molecular dynamics study of oxidized lipid bilayers in NaCl solution, J. Phys. Chem. B 117 (2013) 8490–8501.
[17] M. Afri, H.E. Gottlieb, A.A. Frimer, Superoxide organic chemistry within the liposomal bilayer, part II: a correlation between location and chemistry, Free Radic. Biol. Med. 32 (2002) 605–618.
[18] C.A. Fortier, B. Guan, R.B. Cole, M.A. Tarr, Covalently bound fluorescent probes as reporters for hydroxyl radical penetration into liposomal membranes, Free Radic. Biol. Med. 46 (2009) 1376–1385.
[19] A. Gamliel, M. Afri, A.A. Frimer, Determining radical penetration of lipid bilayers with new lipophilic spin traps, Free Radic. Biol. Med. 44 (2008) 1394–1405.
[20] A. Kyrychenko, A.S. Ladokhin, Molecular dynamics simulations of depth distribution of spin-labeled phospholipids within lipid bilayer, J. Phys. Chem. B 117 (2013) 5875–5885.
[21] M. Roeselová, J. Vieceli, L.X. Dang, B.C. Garrett, D.J. Tobias, Hydroxyl radical at the air–water interface, J. Am. Chem. Soc. 126 (2004) 16308–16309.
[22] R. Vácha, P. Slavíček, M. Mucha, B.J. Finlayson-Pitts, P. Jungwirth, Adsorption of atmospherically relevant gases at the air/water interface: free energy profiles of aqueous solvation of N_2, O_2, O_3, OH, H_2O, HO_2, and H_2O_2, J. Phys. Chem. A 108 (2004) 11573–11579.
[23] J. Vieceli, M. Roeselová, N. Potter, L.X. Dang, B.C. Garrett, D.J. Tobias, Molecular dynamics simulations of atmospheric oxidants at the air–water interface: solvation and accommodation of OH and O_3, J. Phys. Chem. B 109 (2005) 15876–15892.
[24] M.T.C. Martins-Costa, J.M. Anglada, J.S. Francisco, M.F. Ruiz-Lopez, Reactivity of atmospherically relevant small radicals at the air–water interface, Angew. Chem. Int. Ed. 51 (2012) 5413–5417.
[25] Y.-H. Chung, J. Xia, C.J. Margulis, Diffusion and residence time of hydrogen peroxide and water in crowded protein environments, J. Phys. Chem. B 111 (2007) 13336–13344.
[26] L. Domínguez, A. Sosa-Peinado, W. Hansberg, Catalase evolved to concentrate H_2O_2 at its active site, Arch. Biochem. Biophys. 500 (2010) 82–91.
[27] M. Yusupov, A. Bogaerts, S. Huygh, R. Snoeckx, A.C.T. van Duin, E.C. Neyts, Plasma-induced destruction of bacterial cell wall components: a reactive molecular dynamics simulation, J. Phys. Chem. C 117 (2013) 5993–5998.
[28] M.N. Möller, J.R. Lancaster Jr., A. Denicola, The interaction of reactive oxygen and nitrogen species with membranes, in: S. Matalon (Ed.), Current Topics in Membranes, Elsevier, 2008, pp. 23–42.
[29] X. Liu, M.J. Miller, M.S. Joshi, D.D. Thomas, J.R. Lancaster Jr., Accelerated reaction of nitric oxide with O_2 within the hydrophobic interior of biological membranes, Proc. Natl. Acad. Sci. U. S. A. 95 (1998) 2175–2179.
[30] F.M. Engelmann, I. Mayer, D.S. Gabrielli, H.E. Toma, A.J. Kowaltowski, K. Araki, M.S. Baptista, Interaction of cationic meso-porphyrins with liposomes, mitochondria and erythrocytes, J. Bioenerg. Biomembr. 39 (2007) 175–185.
[31] R.M. Cordeiro, R. Miotto, M.S. Baptista, Photodynamic efficiency of cationic meso-porphyrins at lipid bilayers: insights from molecular dynamics simulations, J. Phys. Chem. B 116 (2012) 14618–14627.
[32] S.-J. Marrink, H.J.C. Berendsen, Simulation of water transport through a lipid membrane, J. Phys. Chem. 98 (1994) 4155–4168.
[33] S.-J. Marrink, H.J.C. Berendsen, Permeation process of small molecules across lipid membranes studied by molecular dynamics simulations, J. Phys. Chem. 100 (1996) 16729–16738.
[34] P. Jedlovszky, M. Mezei, Effect of cholesterol on the properties of phospholipid membranes. 2. Free energy profile of small molecules, J. Phys. Chem. B 107 (2003) 5322–5332.
[35] C.L. Wennberg, D. van der Spoel, J.S. Hub, Large influence of cholesterol on solute partitioning into lipid membranes, J. Am. Chem. Soc. 134 (2012) 5351–5361.
[36] M.S. Al-Abdul-Wahid, C.-H. Yu, I. Batruch, F. Evanics, R. Pomès, R.S. Prosser, A combined NMR and molecular dynamics study of the transmembrane solubility and diffusion rate profile of dioxygen in lipid bilayers, Biochemistry 45 (2006) 10719–10728.
[37] M.P. Allen, D.J. Tildesley, Computer Simulation of Liquids, Clarendon Press, Oxford, 2009.
[38] D. Frenkel, B. Smit, Understanding Molecular Simulation: From Algorithms to Applications, Academic Press, San Diego, 2001.
[39] B. Hess, C. Kutzner, D. van der Spoel, E. Lindahl, GROMACS 4: algorithms for highly efficient, load-balanced, and scalable molecular simulation, J. Chem. Theory Comput. 4 (2008) 435–447.
[40] D. van der Spoel, E. Lindahl, B. Hess, G. Groenhof, A.E. Mark, H.J.C. Berendsen, GROMACS: fast, flexible, and free, J. Comput. Chem. 26 (2005) 1701–1718.
[41] D. Poger, A.E. Mark, On the validation of molecular dynamics simulations of saturated and cis-monounsaturated phosphatidylcholine lipid bilayers: a comparison with experiment, J. Chem. Theory Comput. 6 (2010) 325–336.
[42] H.J.C. Berendsen, J.P.M. Postma, W.F. van Gunsteren, J. Hermans, Interaction models for water in relation to protein hydration, in: B. Pullman (Ed.), Intermolecular Forces, Reidel, Dordrecht, 1981, pp. 331–342.
[43] C. Oostenbrink, A. Villa, A.E. Mark, W.F. van Gunsteren, A biomolecular force field based on the free enthalpy of hydration and solvation: the GROMOS force-field parameter sets 53A5 and 53A6, J. Comput. Chem. 25 (2004) 1656–1676.
[44] M. Swart, Density Functional Theory Applied to Copper Proteins, (Ph.D. thesis) Rijksuniversiteit Groningen, Netherlands, September 2002.
[45] J. Koput, S. Carter, N.C. Handy, Potential energy surface and vibrational-rotational energy levels of hydrogen peroxide, J. Phys. Chem. A 102 (1998) 6325–6330.
[46] CRC Handbook of Chemistry and Physics, 84th ed., 2003.
[47] T. Sawyer, J.S. Valentine, How super is superoxide? Acc. Chem. Res. 14 (1981) 393–400.
[48] W.C. Schumb, C.N. Satterfield, R.L. Wentworth, Hydrogen peroxide, ACS Monograph Series, Rheinhold, 1955.
[49] R. Sander, Compilation of Henry's Law Constants for Inorganic and Organic Species of Potential Importance in Environmental Chemistry — Version 3, http://www.henrys-law.org1999(accessed March 2013).
[50] J.D. Wild, T. Sridhar, O.E. Potter, Solubility of nitrogen and oxygen in cyclohexane, Chem. Eng. J. 15 (1978) 209–214.
[51] R. Battino, T.R. Rettich, T. Tominaga, The solubility of oxygen and ozone in liquids, J. Phys. Chem. Ref. Data 12 (1983) 163–178.
[52] A. Roy, P. Carpentier, D. Bourgeois, M. Field, Diffusion pathways of oxygen species in the phototoxic fluorescent protein KillerRed, Photochem. Photobiol. Sci. 9 (2010) 1342–1350.
[53] P.C. Lee, M.A.J. Rodgers, Singlet molecular oxygen in micellar systems. 1. Distribution equilibria between hydrophobic and hydrophilic compartments, J. Phys. Chem. 87 (1983) 4894–4898.
[54] F. Castañeda, A.L. Zanocco, M. Meléndrez, G. Günther, E. Lemp, Useful probes for studying singlet oxygen dynamics and equilibria in microcompartmentalized systems, J. Photochem. Photobiol. A Chem. 168 (2004) 175–183.
[55] A.L. Zanocco, M. Meléndrez, G. Günther, E. Lemp, Study of singlet oxygen equilibrium in dioctadecyldimethylammonium chloride vesicles employing 2-(n-(N, N, N-trimethylamine)-n-alkyl)-5-alkylfuryl halides, Photochem. Photobiol. 83 (2007) 584–591.
[56] V.S. Sokolov, P. Pohl, Membrane transport of singlet oxygen monitored by dipole potential measurements, Biophys. J. 96 (2009) 77–85.
[57] N.M. Garrido, M. Jorge, A.J. Queimada, E.A. Macedo, I.G. Economou, Using molecular simulation to predict solute solvation and partition coefficients in solvents of different polarity, Phys. Chem. Chem. Phys. 13 (2011) 9155–9164.
[58] J. Kästner, Umbrella sampling, WIREs Comput. Mol. Sci. 1 (2011) 932–942.
[59] J.S. Hub, B.L. de Groot, D. van der Spoel, g_wham — a free weighted histogram analysis implementation including robust error and autocorrelation estimates, J. Chem. Theory Comput. 6 (2010) 3713–3720.
[60] E. Cadenas, K.J. Davies, Mitochondrial free radical generation, oxidative stress, and aging, Free Radic. Biol. Med. 29 (2000) 222–230.
[61] F. Fogolari, A. Corazza, S. Toppo, S.C.E. Tosatto, P. Viglino, F. Ursini, G. Esposito, Studying interactions by molecular dynamics simulations at high concentration, J. Biomed. Biotechnol. (2012) 303190.
[62] S.A. Pandit, D. Bostick, M.L. Berkowitz, Molecular dynamics simulation of a dipalmitoylphosphatidylcholine bilayer with NaCl, Biophys. J. 84 (2003) 3743–3750.
[63] R.W. Impey, P.A. Madden, I.R. McDonald, Hydration and mobility of ions in solution, J. Phys. Chem. 87 (1983) 5071–5083.
[64] W.K. Subczynski, J.S. Hyde, Concentration of oxygen in lipid bilayers using a spin-label method, Biophys. J. 41 (1983) 283–286.
[65] J.C. Mathai, V. Sitaramam, Stretch sensitivity of transmembrane mobility of hydrogen peroxide through voids in the bilayer. Role of cardiolipin, J. Biol. Chem. 269 (1994) 17784–17793.
[66] A.F. Uchoa, D. Severino, M.S. Baptista, Antioxidant properties of singlet oxygen supressors, in: C.L. Céspedes, D.A. Sampietro, D.S. Seigler, M. Rai (Eds.), Natural Antioxidants and Biocides from Wild Medicinal Plants, CABI, 2013, pp. 65–91.
[67] B.H.J. Bielski, R.L. Arudi, M.W. Sutherland, A study of the reactivity of HO_2/O_2^- with unsaturated fatty acids, J. Biol. Chem. 258 (1983) 4759–4761.
[68] J.M. Gebicki, B.H.J. Bielski, Comparison of the capacities of the perhydroxyl and the superoxide radicals to initiate chain oxidation of linoleic acid, J. Am. Chem. Soc. 103 (1981) 7020–7022.
[69] K. Fukuzawa, J.M. Gebicki, Oxidation of α-tocopherol in micelles and liposomes by the hydroxyl, perhydroxyl, and superoxide free radicals, Arch. Biochem. Biophys. 226 (1983) 242–251.
[70] R.A. Gus'kova, I.I. Ivanov, V.K. Kol'tover, V.V. Akhobadze, A.B. Rubin, Permeability of bilayer lipid membranes for superoxide (O_2^-) radicals, Biochim. Biophys. Acta 778 (1984) 579–585.
[71] A.D.N.J. de Grey, HO_2: the forgotten radical, DNA Cell Biol. 21 (2002) 251–257.
[72] K. Fukuzawa, Dynamics of lipid peroxidation and antioxidation of α-tocopherol in membranes, J. Nutr. Sci. Vitaminol. 54 (2008) 273–285.
[73] E. Codorniu-Hernández, P.G. Kusalik, Mobility mechanism of hydroxyl radicals in aqueous solution via hydrogen transfer, J. Am. Chem. Soc. 134 (2012) 532–538.